13th World Conference on Earthquake Engineering
Vancouver, B.C., Canada
August 1-6, 2004
Paper No. 1603

SEISMIC RESPONSE AND DESIGN OF POST-TENSIONED STEEL MOMENT RESISTING FRAMES WITH FRICTION COMPONENTS

Pedro ROJAS[1], James M. RICLES[2], and Richard SAUSE[3]

SUMMARY

A post-tensioned friction damped connection (PFDC) for earthquake resistant steel moment resisting frames (MRFs) is introduced. The connection includes friction components on the beam flanges with post-tensioned (PT) high strength strands running parallel to the beam. The connection minimizes inelastic deformation to the connection components and requires no field welding. Nonlinear analyses were performed on a 6-story, 4-bay steel MRF with PFDCs to study its response to strong ground shaking. A performance based design approach was developed to design the PFDC-MRF. The results demonstrate that the seismic performance of a PFDC-MRF is satisfactory in terms of strength, energy dissipation, deformation, and self-centering capability. The analysis indicate that the seismic performance of a PFDC frame can exceed that of a frame with conventional moment resisting connections.

INTRODUCTION

During the 1994 Northridge Earthquake, many steel-framed buildings suffered unexpected premature fractures in their welded beam-to-column connections. The occurrence of these premature fractures forced the engineering community to revise design and construction practice. Recent research has provided new details for MRF construction, but these new details are expensive to fabricate. Moreover, the use of the standard MRF connection often results in damage and permanent drift in the MRF following a major earthquake.

As an alternative to welded construction, a post-tensioned friction damped connection (PFDC) for use in seismic resistant steel MRFs was developed. The connection utilizes high strength steel strands (Figure 1(a)) that are post-tensioned after the friction components are installed. The post-tensioning strands run through the column, and are anchored outside the connection region (Figure 1(b)). A properly designed PFDC has several advantages: (1) field welding is not required; (2) the connection is made with conventional materials and skills; (3) the connection has an initial stiffness similar to that of a typical

[1] Professor, Catholic University, Ecuador, per2@ecua.net.ec
[2] Professor, Lehigh University, jmr5@lehigh.edu
[3] Professor, Lehigh University, rs0c@lehigh.edu

welded connection; (4) the connection is self-centering without permanent deformation, thus the MRF will not have residual drift after an earthquake if significant residual deformation does not occur at the base of the ground floor columns; and (5) the columns and beams remain essentially elastic while the friction plates provide energy dissipation.

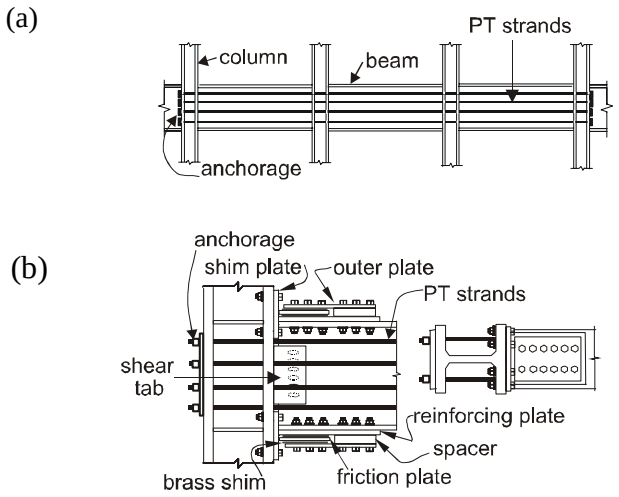

Figure 1. Schematic elevation of (a) one floor of a MRF with PFDCs and (b) connection details.

This paper describes the details, behavior, design approach, and analytical studies of a steel MRF with PFDCs. This type of frame is herein referred to as a PFDC-MRF. Experimental test results were used to calibrate a fiber element connection model, which in turn was used to analyze a 6-story, 4-bay steel PFDC-MRF. Nonlinear static and dynamic analyses were performed using the model and the results were compared to the results of a MRF with standard fully restrained welded connections (FR-MRF). The actual seismic response of the PFDC-MRF was also compared to the estimated response, which was based on the design approach developed for PFDC-MRFs.

PREVIOUS RESEARCH

The development of PDFCs utilizes three areas of related existing construction technologies: post-tensioned (PT) precast concrete construction, PT steel MRF connections, and passive frictional dampers.

Experimental and analytical studies of PT precast concrete connections were conducted by several researchers (e.g., El-Sheik [1]). The results from these studies show that these types of connections are well suited for seismic resistant precast concrete structural systems.

Experimental and analytical studies at Lehigh University investigated the behavior of an innovative PT wide flange beam-to-column moment connection with top-and-seat angles for steel MRFs (Garlock [2], Ricles [3], Ricles [4]). The results show that the PT steel connections can provide adequate strength and stiffness for a MRF subjected to strong ground shaking.

Friction dampers have been used to improve the seismic performance of panel and braced structures in Canada. The improvement in performance is mainly due to the increase in energy dissipation provided by the friction dampers, which reduces the damage to the primary elements of the structure. Petty [5] carried out preliminary studies of PT connections with friction devices located at the beam web. The studies

involved experiments on the cyclic behavior of the friction connection component (FCC). Petty's results show that friction is a viable way to dissipate energy in a PT steel connection.

POST-TENSIONED FRICTION DAMPED CONNECTION

Connection details

As mentioned previously, a PFDC has post-tensioned (PT) high strength strands running parallel to the beam and anchored outside of the connection (Figure 1). Due to the initial post-tensioning force applied to the strands, the beam flanges are compressed against the column flanges. As shown in Figure 1(b), reinforcing plates are placed on the beam flanges to limit beam compression yielding and thus, to minimize structural damage. Shim plates are placed between the column flange and the beam flanges so that only the beam flanges and reinforcing plates are in contact with the column, thereby protecting the beam web from yielding under bearing stress.

Friction devices are located at the beam flanges (Figure 1(b)). The devices consist of a friction plate sandwiched by two brass shim plates that are inserted between the beam flange reinforcing and outer plates. All plates are bolted to the beam flanges. Long slotted holes are drilled in the friction plate. The friction plate is attached to a tee flange that also serves as a shim plate (i.e., the friction plate is the tee stem, see Figure 1(b)). Friction is generated when the beam flanges and outer plate slide against the "stationary" friction plate when the beam rotates about the center of rotation situated at the mid-depth of the reinforcing plates (see Figure 2 insert). The brass shim plates are used to produce a stable friction force and to mantain the energy dissipation capacity of the PFDC (Petty [5]). A shear tab is bolted to the beam web (with slotted holes) and welded to the column flange to transmit the beam gravity shear forces. Slotted holes in the friction plate enable the beam flange and outer plate to slide relative to the friction plate in an uninhibited manner. The slotted holes in the beam web allow the beam to rotate relative to the column flange without damage to the shear tab. The beam vertical shear in excess of the gravity shear is resisted by friction forces at the beam-column interface where the beam flange is compressed against the column flange.

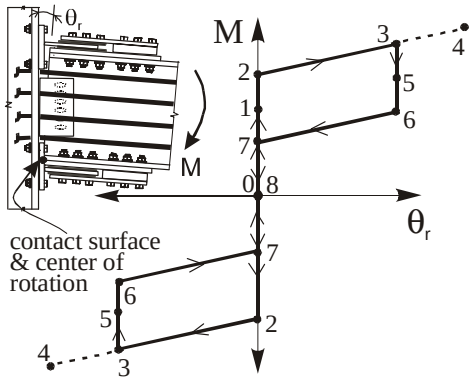

Figure 2. Idealized moment-relative rotation behavior of a PFDC.

Flexural Behavior

Figure 2 shows the idealized moment-relative rotation (M-θ_r) curve for a PFDC when subjected to cyclic loading. The behavior is characterized by gap opening (θ_r) and closing at the beam-column interface. Under applied moment, the connection initially behaves as a fully restrained connection, where the initial stiffness is similar to that of a fully restrained welded moment connection when θ_r is equal to zero (events 0 to 2 in Figure 2). Once the magnitude of the applied moment reaches the moment resistance provided by

the initial PT force in the strands, which clamps the beam against the column, *decompression* of the beam from the column face (shim plate) occurs. The applied moment continues to increase between events 1 and 2 as the rotation of the beam is restrained by the resistance of the friction component at the beam tension flange. At point 1 the friction force is minimal and increases gradually up to its maximum value (computed using Coulomb friction theory) at event 2, which is the point of *incipient rotation*. At incipient rotation a gap opening occurs between the column face and beam tension flange.

The stiffness of the connection after gap opening is associated with the elastic axial stiffness of the PT strands. With increased loading, the strands elongate, producing an additional force, which contribute to resist the total applied moment. Yielding of the strands eventually may occur at event 4. Upon unloading (event 3), θ_r remains constant between events 3 to 6 until the frictional force under load reversal in the friction plates is overcome at event 6. Between events 6 and 7, the beam rotates until the beam decompressed tension flange is back in contact with the shim plate. Between events 7 and 8 the beam is compressed against the shim plates. A complete reversal in the applied moment will result in a similar connection behavior occurring in the opposite direction of loading, as shown in Figure 2.

As long as the strands remain remain elastic, and there is no significant beam yielding, the post-tensioning force is preserved and the connection will self-center upon unloading. The energy dissipation capacity of the connection is related to the friction force.

Moment Capacity of the Connection

The moment capacity of the connection can be determined considering the free body diagram of Figure 3 as follows

$$M = d_1 F_f + P d_2 \tag{1}$$

where F_f is the maximum friction force assumed to be acting at the mid-depth of the friction plate attached to the beam tension flange, P is the beam axial force, and d_1 and d_2 are the distances from the line of actions of F_f and P to the contact force C of the beam compression flange reinforcing plate, respectively. The contact force C is assumed to act at the mid-depth of the reinforcing plate (i.e., at the center of rotation of the connection).

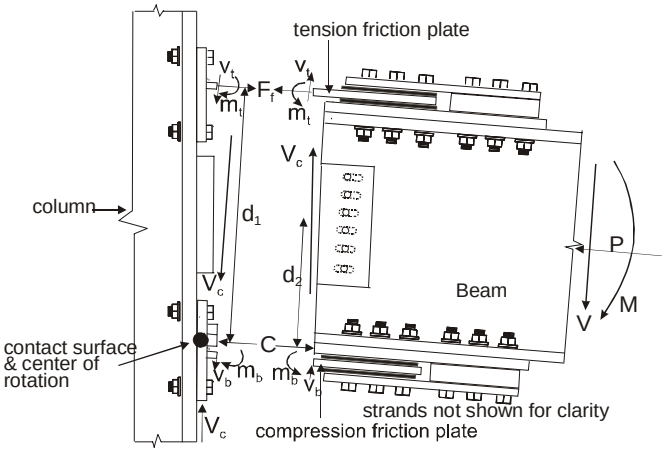

Figure 3. Free body diagram of a PFDC.

The values of F_f, P, and C are estimated using Equations (2), (3), and (4), respectively.

$$F_f = 2\mu N \tag{2}$$

$$P = T + F_{fd} \tag{3}$$

and

$$C = P + F_f \tag{4}$$

where μ is the friction coefficient, N is the normal force generated by the pretensioned bolts placed through the slotted holes of the friction plates between the tribo surfaces, and the factor 2 is due to the presence of two sliding surfaces on each friction plate. In Equation (3), T is the post-tensioning strand force and F_{fd} is an additional beam axial force, produced by the interaction of the PFDC frame with the floor diaphragm (further details about this interaction can be found in Rojas [6]). The value of T is given by Equation (5) as follows:

$$T = T_o + 2d_2\left(\frac{k_b k_s}{k_b + k_s}\right)\theta_r \tag{5}$$

where T_o is the sum of the initial post-tensioning force in all strands, k_s and k_b are the total strand stiffness and beam axial stiffness, respectively, and d_2 and θ_r were defined above.

PROPOSED SEISMIC DESIGN APPROACH FOR PFDC-MRFs

A performance based design approach was developed for PFDC-MRFs. The design approach uses two seismic performance levels: (1) the "immediate occupancy" performance level, which describes a post-earthquake damage state in which only limited structural and non-structural damage has occurred; and (2) the "collapse prevention" performance level, which describes a post-earthquake damage state in which the building is on the verge of partial or total collapse. The design approach considers two earthquake ground motion levels: (1) the design basis earthquake (DBE); and (2) the maximum considered earthquake (MCE). The MCE has a 2% probability of being exceeded in 50 years while the DBE is defined as 2/3 the intensity of the MCE, with an approximate 10% probability of being exceeded in 50 years.

Design Objectives

The proposed design approach for PFDC-MRFs has two objectives: (1) to achieve the immediate occupancy level under DBE ground motions; and (2) to achieve the collapse prevention level under MCE ground motions. Under DBE ground motions, the structural components of the PFDC system should not develop inelastic behavior, except for minimal yielding in the beam flanges at the end of the reinforcing plates. As a result, the building is ready to be reoccupied after the DBE. The PT strands and friction devices are designed to remain elastic under MCE ground motions. Some inelastic behavior is expected in the panel zones, beams, and columns, with the onset of local buckling occurring in a few of the beams. With an appreciable amount of local beam buckling, a loss of post-tensioning would occur leading to a degradation in frame capacity. Thus, under MCE ground motions, the frame is expected to loose its self-centering capacity, but not collapse.

Structural Demands

In order to meet the design objectives, the structural demands in the PFDC-MRF at the DBE and MCE levels must be estimated. These estimated structural demands are determined using an *amplified-code*

based procedure that uses the *equal displacement principle* between an elastic and inelastic structure to estimate the roof drift, θ_{roof}, (roof displacement divided by the total height of the frame) of the frame given the design base shear (V_{des}). V_{des} is the design base shear as recommended by the 2000 International Building Code [7]. The estimated story drift (θ) at the DBE and MCE levels is estimated from the roof drift as follows

$$\theta_{DBE} = C_\theta \theta_{roof,DBE} \tag{6a}$$

$$\theta_{MCE} = C_\theta \theta_{roof,MCE} \tag{6b}$$

where C_θ is equal to 1.5 and based on results of nonlinear dynamic analyses of the PFDC frame performed by Rojas [6]. Figure 4(a) shows the story drifts and the corresponding base shears at the DBE and MCE levels (V_{DBE} and V_{MCE}). V_{DBE} and V_{MCE} are related to V_{des} by the overstrength factors Ω_{DBE} and Ω_{MCE}, respectively, which are a function of the connection design. If the elastic component of story drift ($\theta_{el,DBE}$ and $\theta_{el,MCE}$), shown also in Figure 4(a), is substracted from the total story drift, the connection relative rotation (θ_r) can be expressed as

$$\theta_{r,DBE} = \theta_{DBE} - \frac{V_{DBE}}{K_{f\theta}} \tag{7a}$$

$$\theta_{r,MCE} = \theta_{MCE} - \frac{V_{MCE}}{K_{f\theta}} \tag{7b}$$

where the stiffness $K_{f\theta}$ can be easily determined from the initial stiffness of the PFDC frame. Once θ_r is known, the parameters needed to design a PFDC-MRF can be estimated, since the design parameters are directly or indirectly related to θ_r. Figure 4(b) shows the relative rotations and the corresponding connection strengths at both ground motion levels (M_{DBE} and M_{MCE}). Figure 4(b) also shows the connection strengths at decompression and imminent gap opening (M_d and M_{IGO}) and the design moment (M_{des}), where the latter is obtained from an equivalent lateral force procedure with the design base shear equal to V_{des}. The shape of the M-θ_r curve is controlled by the connection design, including: beam depth, beam axial force, initial post-tensioning force, number and elastic axial stiffness of the post-tensioned strands, maximum friction force, and the strength of the connection components relative to the total connection capacity.

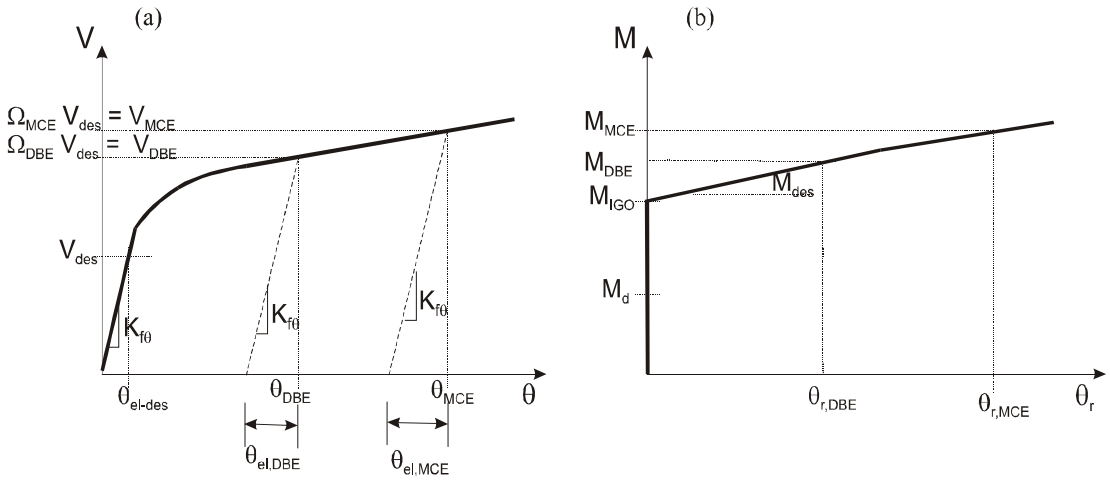

Figure 4. Estimated structural demands: (a) global level and (b) local level.

PFDC ANALYTICAL MODELING

An analytical model of a PFDC and the associated beams and columns was developed using the DRAIN-2DX computer program (Prakash [8] and Herrera [9]). Figure 5 shows the analytical model. The beams and columns are modeled using fiber elements that are divided into a number of segments along the element length. Only one segment is used in those elements where linear elastic behavior is expected. The cross-section of each segment is comprised of several fibers. A material stress-strain relationship, a cross sectional area, and a distance from the longitudinal reference axis of the member characterize each fiber. The beam fiber elements adjacent to the column are used to model connection gap opening. The fibers of the beam cross section initially in contact with the shim plates are assigned a stress-strain relationship that has stiffness in compression, but none in tension. Fibers are omitted from the cross section not in contact with the shim plates. More details about the model can be seen in Rojas [6].

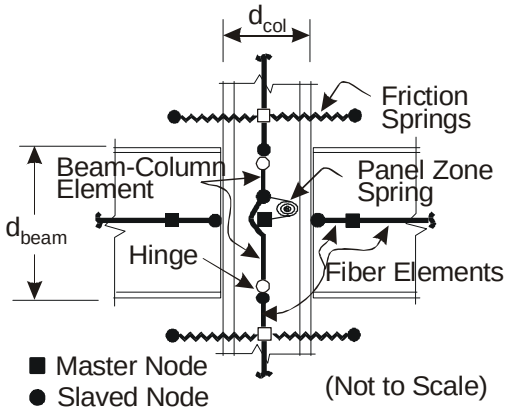

Figure 5. PFDC analytical model.

As seen in Figure 5, the panel zone region is modeled using a set of master-slave nodes. The panel zone flexibility was modeled by placing two rotational springs (identified as panel zone springs in Figure 5) with moment-rotational characteristics determined from the shear force-shear deformation behavior of the panel zone (Rojas [6]). The strands and friction devices were modeled using truss elements and spring elements having a rigid-plastic force deformation relationship, respectively.

SEISMIC BEHAVIOR OF PFDC-MRF

Description and Design of Frames

A 6-story, 4-bay perimeter MRF was designed as a PFDC-MRF in accordance with the procedure described previously. A second 6-story, 4-bay perimeter special MRF with welded connections (referred to as FR-MRF) was also designed using the IBC 2000 provisions. The following assumptions were made to design both frames: (1) IBC 2000 equivalent lateral load procedure for special MRFs was applicable; (2) the structure is an office building located on stiff soil in the Los Angeles area; (3) the design accelerations were determined using the deterministic limit of the IBC 2000 site-specific procedure; and (4) A992 steel sections were used. The member sizes for both frames are shown in Figure 6. It is seen that the beams of the PFDC frame are larger than the beams of the FR frame since the beams of the PFDC frame have to carry axial load in addition to bending moment. On the contrary, the columns of the FR frame are larger than those of the PFDC frame since the moments developed in a welded moment connection of the FR frame are larger than those developed in a PFDC.

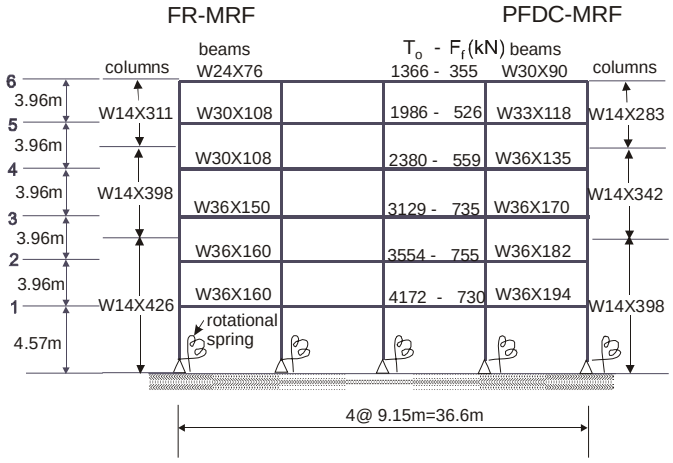

Figure 6. Frames used in analytical study.

For the design of the PFDC-MRF, the target values of M_{IGO}/M_{des} = 0.95, M_{DBE}/M_{des} = 1.50, and M_{MCE}/M_{des} = 1.80 were used. The values are the result of several studies by Garlock [10] and Rojas [6] on MRFs with post-tensioned connection, where these MRFs performed well under seismic loading. The PFDCs were designed at $\theta_{r,DBE}$ of 0.018 radians with a flexural capacity ranging between 0.88 to 0.95$M_{p,n}$ (where $M_{p,n}$ is the nominal plastic moment of the beam). The reinforcing plates were 1829 mm long. Figure 6 indicates the initial post-tensioning (T_o) and the maximum friction forces (F_f) provided in the PFDC-MRF. The values for F_f were determined using a friction coefficient, μ, of 0.40, resulting in a reasonable number of bolts through the friction plates. The contribution of the strands to the total connection capacity was about 80%. More details can be found in Rojas [6].

Analytical Model of Frames

A DRAIN-2DX model of each frame was created with the member sizes shown in Figure 6. One model had rigid connections and the other had PDFCs. The beams, columns, and panel zones of both frames were modeled as described in the model with PFDCs (except that the details related to gap opening, post-tensioning, and friction devices were omitted in the FR-MRF). A beam plastic hinge model that includes strength degradation and strain hardening was implemented to model local buckling in the FR-MRF (Rojas [6]). P-delta effects from the building interior gravity frames were incorporated into the FR-MRF

and PFDC-MRF models using a leaning column. Gravity loads (unfactored) were applied to the MRFs and the leaning column of both frames. The flexibility of the foundation was also taken into account in both models.

The initial post-tensioning in the PFDC-MRF was applied using the DRAIN-2DX option for "element loads", which imposes an initial stress condition. The interaction between the floor diaphragm system and the PFDC–MRF was also included via springs that model the strength and the stiffness of three collector beam elements, which are connected to the three central columns of the PFDC-MRF. The collector beam elements transfer the inertia forces from the floor diaphragms to the PFDC-MRF. The additional beam axial force (F_{fd}), described previously (see Equation 3) enters the PFDC frame via the springs that represent the collector beam elements.

Static Pushover Analysis Results

A Nonlinear Static Pushover Analysis was performed for each frame. The lateral loads were distributed over the height of the frames in accordance with the IBC 2000 provisions and were applied at the mass locations of both frames. Figure 7 shows the relationship between the normalized base shear (base shear divided by the seismic dead weight of the frame, W) and the roof drift, θ_{roof}, for both frames. The analysis results for the FR-MRF show that first yielding occurs when the base shear is 0.13W (θ_{roof} = 0.95%). The maximum overstrength, Ω_o, of the FR-MRF is 3.14 (equivalent to 0.21W) at a corresponding θ_{roof} of 2.50%. The overstrength is defined as the base shear divided by the IBC 2000 design base shear. At the roof drift, θ_{roof}, of 5%, the maximum story drift, θ, is 5.99% and occurs at the first story. Inelastic behavior occurs in the beams of all floors, at the base of the first story columns, and in most of the interior panel zones.

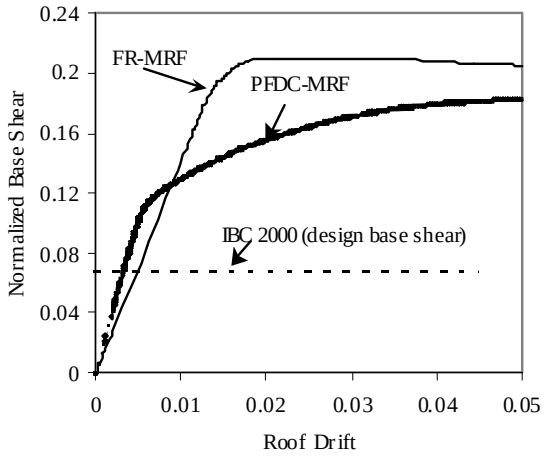

Figure 7. Static Pushover Results.

As seen from Figure 7, the PFDC-MRF has a larger initial stiffness than the FR-MRF due to the larger beam sections and reinforcing plates. The first connection gap opening occurs at a base shear of 0.0564W (θ_{roof} = 0.27%). The beginning of a significant reduction in the PFDC-MRF lateral stiffness occurs at a base shear of 0.106W (θ_{roof} = 0.53%) due to gap opening of several connections. First yielding occurs at the base of the first story columns when the base shear is 0.13W and θ_{roof} is 1.11%. The maximum overstrength of the PFDC-MRF is 2.73 (0.18W) when θ_{roof} is 5%. At the roof drift, θ_{roof}, of 5%, the maximum story drift is 6.18% and occurs at the first story. Beam compression yielding at the ends of the

reinforcing plates begin when θ_{roof} is 1.90%. The panel zones remain essentially elastic. No inelastic behavior occurs in the strands.

Time History Analysis Results

Ground Motions

An ensemble of eight records was used to investigate the seismic behavior of the FR-MRF and PFDC-MRF. Two sets of analyses were conducted. For one set of analyses, the eight ground motions were scaled to the DBE level. For the second set, the eight records were scaled to the MCE level. The scaling procedure developed by Somerville [11] was used, with the IBC 2000 DBE and MCE response spectra as the target spectra. The IBC 2000 DBE and MCE response spectra are compared to the response spectra for the eight DBE level scaled ground motions in Figure 8. The fundamental elastic period, T_1, of the frames are 2.03 and 1.74 seconds for the FR-MRF and PFDC-MRF, respectively.

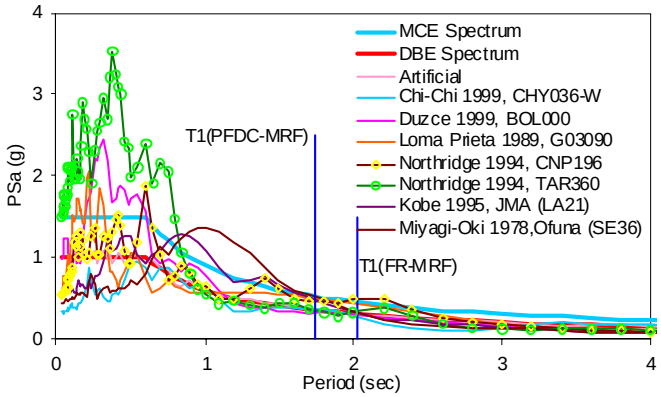

Figure 8. Response spectra.

Global Response

The mean, *m*, and mean plus one standard deviation, $m+\sigma$, of the maximum story drifts at each story are shown in Figure 9. It is noted that here, and throughout the paper, the mean, *m*, and mean plus one standard deviation, $m+\sigma$, are statistical results over the eight ground motions. The results in Figure 9 indicate that under the DBE ground motions, the FR-MRF drifts more than the PFDC-MRF in the upper stories while in the lower stories the PFDC-MRF drifts more than the FR-MRF. For the MCE ground motions, the PFDC-MRF drifts more than the FR-MRF in all stories.

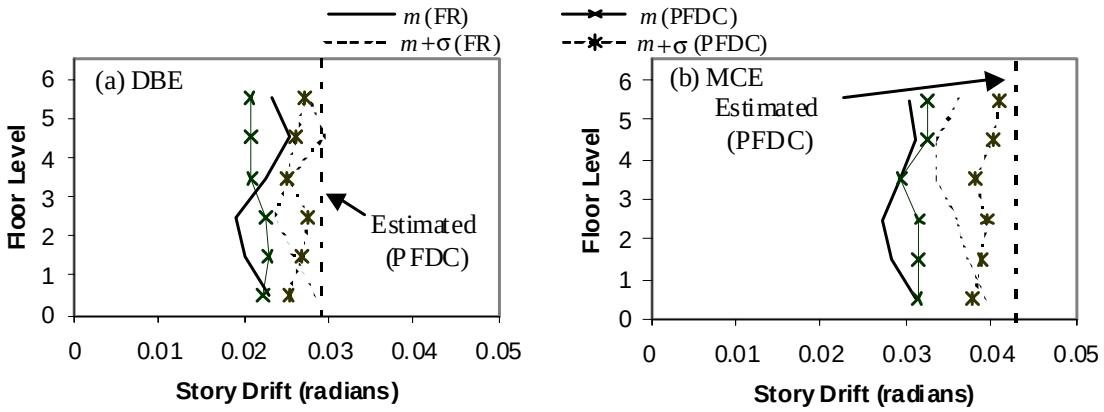

Figure 9. Maximum story drifts for DBE and MCE records.

The self-centering capability of the PFDC-MRF is shown in Figure 10. The PFDC frame shows negligible residual story drift, which means that inelastic behavior (damage) is minimal. The maximum m and $m+\sigma$ values are 0.07% and 0.11%, respectively, for the DBE records; and 0.14% and 0.26%, respectively, for the MCE records. The maximum values always occur in the first story due to yielding at the base of the first story columns. On the contrary, the FR-MRF shows significant residual story drift due to the appreciable inelastic deformations that develop in the structure. The maximum m and $m+\sigma$ values are 0.30% and 0.52%, respectively, for the DBE records; and 0.68% and 1.27%, respectively, for the MCE records. The roof displacement time-history for the PFDC-MRF and FR-MRF to the 1999 Chi-Chi earthquake scaled to the MCE level is shown in Figure 11(a). It can be seen that during the last 30 seconds of the ground motion, the FR-MRF oscillations persist and the residual roof displacement is still quite large (81.2mm), while the PFDC-MRF shows a reduced response and self-centers. Figure 11(b) shows the floor residual displacement profile for both frames at the end of the analysis, with the frames in static equilibrium. The FR-MRF has significant permanent deformation in the upper stories while the PFDC-MRF has negligible residual deformation.

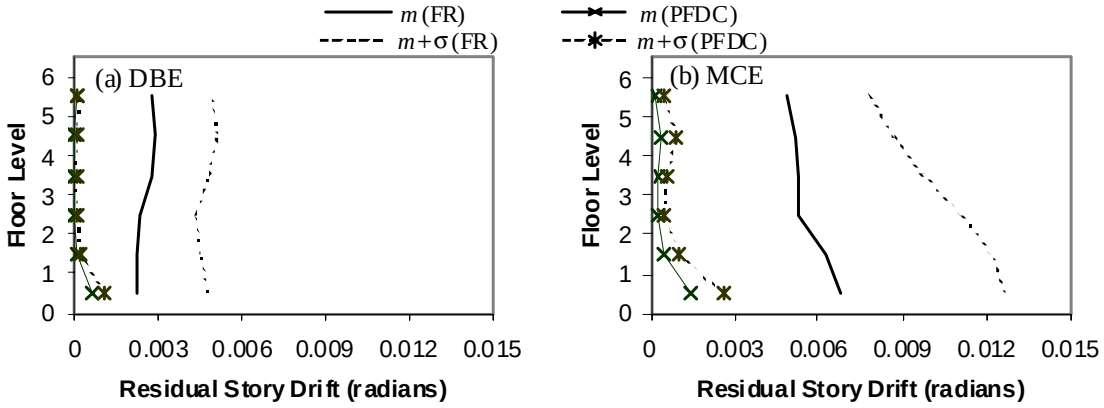

Figure 10. Maximum residual story drifts for DBE and MCE records.

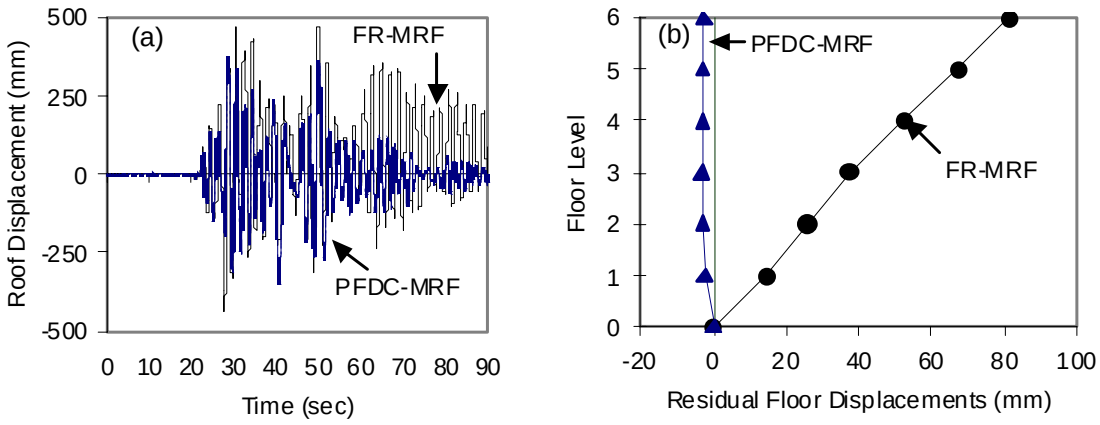

Figure 11. Response of frames to the Chi-Chi MCE ground motion.

In the analyses performed, the PFDC-MRF did not always develop a smaller magnitude of maximum drift response to the selected ground motions. However, even in the cases where the FR-MRF exhibited a smaller magnitude of response, the PFDC-MRF exhibited better behavior that included self-centering with minimal inelastic deformation to the main structural components of the system.

Local Response

Figure 12 compares, for the Miyagi-Oki MCE ground motion, the $M/M_{p,n}$ - θ_p response of an interior connection (located in Floor 5) in the FR-MRF to the $M/M_{p,n}$ - θ_r response of the same connection in the PFDC prototype frame. M is the connection moment, $M_{p,n}$ is the nominal plastic moment capacity of the beam, and θ_p is the beam plastic rotation. It is seen that the connection in the FR-MRF develops larger moments and smaller plastic rotations than the connection in the PFDC-MRF. These results are typical.

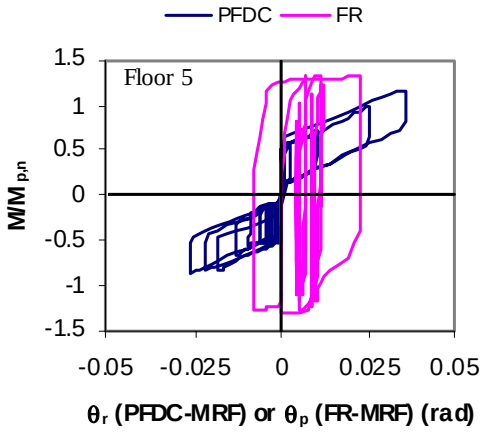

Figure 12. Interior Connection behavior of PFDC and FR-MRFs under the Miyagi MCE ground motion.

The strands in the PFDC-MRF remain elastic under the DBE and MCE records. The panel zones remain essentially elastic under the DBE records while some inelastic behavior was observed under the MCE

records. The beam flanges at the ends of the reinforcing plates developed minor yielding under the DBE records. The yielding at this location was larger for some of the MCE records in a few beams of the frame and possibly local buckling may occur. The inelastic behavior under the DBE and MCE records in the PFDC-MRF was concentrated mainly at the base of the first story columns and in several collector beams. The inelastic behavior in the FR-MRF was in most of the beams, interior panel zones, and at the base of the first story columns.

Seismic Performance of the PFDC-MRF

The conformance of the PFDC-MRF performance to the design objectives was examined by looking at the limit states reached in each time-history analysis (Rojas [6]). From the examination of these limit states, briefly summarized above, it is observed that although the PFDC-MRF did not satisfy some of the design objectives for the DBE ground motions (some yielding occurred at the base of the first story columns), the PFDC-MRF performed well under both the DBE and MCE ground motions. Under the MCE ground motions, the self-centering capability of the PFDC-MRF remained intact. The performance of the PFDC-MRF was satisfactory in terms of strength, energy dissipation, deformation, and self-centering capability.

Estimated and actual response

A comparison of the estimated PFDC-MRF story drift (used in the design procedure) with the time history analysis results is presented in Figure 9. The comparison indicates that the estimated values for story drift are conservative (i.e., they exceed the $m+\sigma$ results for the PFDC-MRF).

The estimated $M/M_{p,n}$ based on Equation 1 and θ_r based on Equation 7 of the design procedure described previously are compared with the time history results in Figures 13 and 14. From Figure 13, it is seen that for the interior bays, the estimated values of $M/M_{p,n}$ are closer to the $m+\sigma$ than the m of the time history results at both ground motion levels. It is also seen that for the exterior bays, the estimated values of $M/M_{p,n}$ agree better with the m of the time history results at both ground motion levels. From Figure 14, it is seen that for the exterior bays, the estimated values for θ_r agree reasonably well with m of the time history results at both ground motion levels. However, it overestimates the m of the time history results of the interior bays at both ground motion levels. For practical purposes (design, fabrication and erection), the design of the exterior connections of the PFDC-MRF was similar to that of the interior connections. The interior bays had a larger design moment.

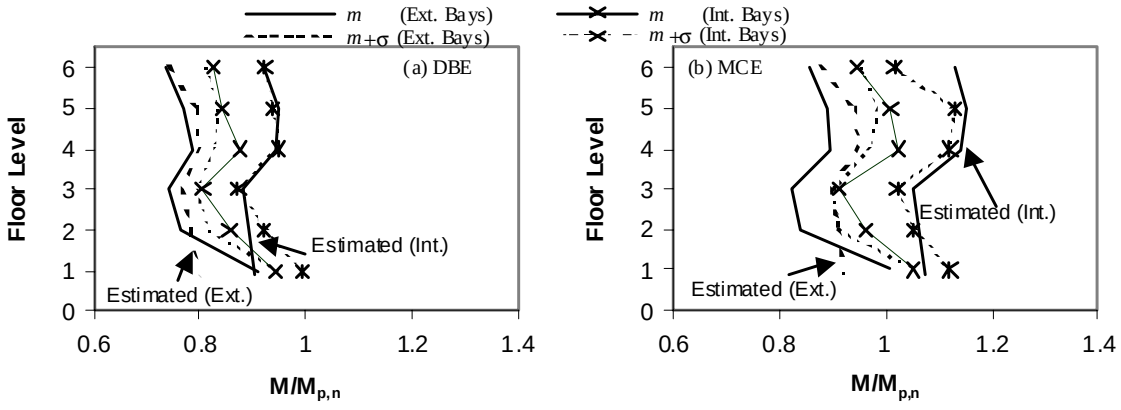

Figure 13. Maximum connection normalized moment from time-history analyses: (a) DBE ground motions, and (b) MCE ground motions; PFDC-MRF.

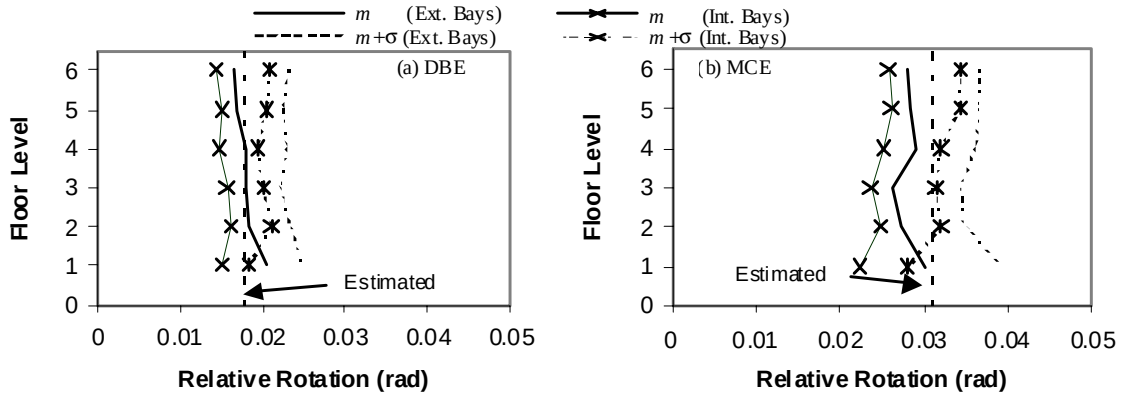

Figure 14. Maximum relative rotations from time-history analyses: (a) DBE ground motions, and (b) MCE ground motions; PFDC-MRF.

SUMMARY AND CONCLUSIONS

An innovative connection for seismic resistant of steel MRFs that requires no field welding has been introduced. Combining high strength PT steel strands with friction devices results in a connection with an initial stiffness that is similar to fully welded moment resisting connections. In addition, the connection has a self-centering capability, resulting in minimal permanent story drift in a building following a severe earthquake. Adequate design of reinforcing plates in beam flanges and doubler plates in panel zones will avoid damage in these elements.

An analytical model based on fiber elements was developed which accurately predicts the behavior of a post-tensioned friction damped connection (PFDC) under cyclic loading. A performance based design approach was used to design a PFDC-MRF. Results from the analytical studies indicate that PFDC-MRFs may perform better than FR-MRFs with welded connections. The seismic performance of a PFDC-MRF was shown to be satisfactory in terms of strength, energy dissipation, deformation, and self-centering capability. In general, most of the design objectives were satisfied, and since the PFDC-MRF performed well suggests that the design approach for PFDC-MRFs is adequate. Although yielding developed at the base of the first story columns, the self-centering capability of the frame was not impaired, especially under the DBE records. The performance under the MCE records was better than anticipated, with controlled inelastic deformations occurring and the self-centering remaining.

ACKNOWLEDGMENTS

The research reported herein was supported by a grant from the Ecuadorian government through a fellowship to the first author, and by a grant from the Pennsylvania Department of Community and Economic Development through the PITA program. The opinions expressed in this paper are those of the authors and do not necessarily reflect the views of the sponsors. The authors would like to thank Professor Maria Garlock for her valuable recommendations related to the research that this paper is based upon.

REFERENCES

1. El-Sheik, M., Sause, R., Pessiki, S., Lu, L.W., and Kurama, Y. "Seismic Analysis, Behavior, and Design of Unbonded Post-Tensioned Precast Concrete Frames." Report No. EQ-97-02, Dept of Civil and Environmental Eng., Lehigh University, Bethlehem, PA., 1997.
2. Garlock, M., Ricles, J., and Sause, R. "Experimental Studies on Full-Scale Post-Tensioned Seismic-Resistant Steel Moment Connections." Proceedings of the 7th U.S. National Conference on Earthquake Engineering (NCEE), Boston, MA., 2002.
3. Ricles, J., Sause, R., Peng, S.W., and Lu, L.W. "Experimental Evaluation of Earthquake Resistant Posttensioned Steel Connections." Journal of Structural Engineering, ASCE, 128(7), 850-859, 2002.
4. Ricles, J., Sause, R., Garlock, M, and Zhao, C. "Post-Tensioned Seismic Resistant Connections for Steel Frames." Journal of Structural Engineering, ASCE, 127(2), 113-121, 2001.
5. Petty, G.D. "Evaluation of a Friction Component for a Post-Tensioned Steel Connection." M.S. Thesis, Civil and Environmental Eng. Dept., Lehigh University, 328pp., 1999.
6. Rojas, P. "Seismic Analysis, Design, and Evaluation of Post-Tensioned Friction Damped Connections for Steel Moment Resisting Frames." Ph.D. Dissertation, Civil and Environmental Eng. Dept., Lehigh University, Bethlehem, PA., 2003.
7. ICC. "International Building Code." International Code Council (ICC), Falls Church, VA., 2000.
8. Prakash, V., Powell, G., and Campbell, S. "DRAIN-2DX Base Program Description and User Guide, Version 1.0." Report No. UCB/SEMM-93/17 & 18, Structural Engineering Mechanics and Materials, Dept. of Civil Engineering, University of California, Berkeley, CA, December, 1993.
9. Herrera, R., Sause, R., and Ricles, J. "Refined Connection Element (Type 05) for DRAIN-2DX, Element Description and User Guide." ATLSS Report No. 01-07, 2001.
10. Garlock, M. "Full-Scale Testing, Seismic Analysis, and Design of Post-Tensioned Seismic Resistant Connections for Steel Frames." P.h.D. Dissertation, Civil and Environmental Eng. Dept., Lehigh University., 2002.
11. Somerville, P. "Development of Ground Motion Time Histories for Phase 2 of the FEMA/SAC Steel Project." Report No. SAC/BD-97/04.AISC. (2000), 1997.